

# Comparative electrochemical behaviour of CO<sub>2</sub> on Pt and Rh electrodes in acid solution

M.L. Marcos<sup>a</sup>, J. González-Velasco<sup>a</sup>, A.E. Bolzán<sup>b</sup>, A.J. Arvia<sup>b,\*</sup>

<sup>a</sup> Departamento de Química, Universidad Autónoma de Madrid, Cantoblanco, 28049 Madrid, Spain

<sup>b</sup> Instituto de Investigaciones Fisicoquímicas Teóricas y Aplicadas (INIFTA), Facultad de Ciencias Exactas, Universidad Nacional de La Plata, Sucursal 4, Casilla de Correo 16, (1900) La Plata, Argentina

Received 7 November 1994; in revised form 6 April 1995

## Abstract

The electroformation of adsorbed species on Pt and Rh from CO<sub>2</sub> dissolved in aqueous 0.5 M H<sub>2</sub>SO<sub>4</sub> and the influence of adsorbed species on the hydrogen evolution reaction (HER) were examined for smooth and columnar structured Pt and smooth and rhodized Rh electrodes at 25°C. Different electroadsorbed species resulting from the adsorption of CO<sub>2</sub> on Rh were found. The electro-oxidation of these adsorbates on Rh takes place over a potential range larger than that for adsorbates on Pt, overlapping the potential range of electroformation of the O-containing layer. A part of the reduced CO<sub>2</sub> adsorbates on Rh behaves as CO-like adsorbates. The presence of adsorbed species from CO<sub>2</sub> influences differently the stationary HER current potential curves for both types of Pt and Rh electrodes. In the range of low current density (cd), the Tafel slope for Pt is  $-0.030$  V decade<sup>-1</sup>. Conversely, the presence of a chemisorbed species on Rh changes the Tafel slope for the HER in the range of low cd from  $-0.030$  V decade<sup>-1</sup> for CO<sub>2</sub>-free solutions to  $-0.120$  V decade<sup>-1</sup> for CO<sub>2</sub>-saturated solution. These changes are explained by a modification in the rate-determining step of the HER produced by chemisorbed species.

**Keywords:** CO<sub>2</sub> electrochemistry; Acid solutions

## 1. Introduction

A few decades ago the formation of a “reduced” carbon dioxide adsorbate (r-CO<sub>2</sub>) on Pt in acids was found, in particular when the electrode–CO<sub>2</sub> interaction took place in the potential range of H-atom electroadsorption [1]. The formation of r-CO<sub>2</sub> adsorbates was of special interest for the electro-oxidation of those organics which could be used as potential fuels in electrochemical energy conversion devices. More recently, the study of the structure and the electrochemical behaviour of r-CO<sub>2</sub> adsorbates was undertaken to establish the reaction pathways related to the production of valuable organics from CO<sub>2</sub> electroreduction [2,3], a process involving waste material

whose accumulation in the atmosphere has been the subject of extensive discussion and concern [4].

Pt and Rh are active electrocatalysts for a number of reactions in aqueous and non-aqueous solutions, but they differ in their behaviour for H-atom electroadsorption, and CO<sub>2</sub> electroreduction and electro-oxidation [5–9]. These differences can be related to the fact that Rh catalysts are very active for the selective synthesis of a number of organic compounds from CO and H<sub>2</sub> [10,11]. Otherwise, the formation of CO<sub>2</sub> adsorbates is largely favoured on H-adsorbing metals such as Pt and Rh, in contrast to Ir, Ru and Os [12]. Similar types of adsorbate are formed probably on Pd electrodeposits as CO<sub>2</sub> electrochemical reduction also takes place on this metal in alkaline solution [13]. Therefore, to understand the electrocatalytic differences between Rh and Pt it is interesting to study comparatively the electro-oxidation characteristics of both r-CO<sub>2</sub> adsorbates and the hydrogen evolution reaction (HER) on these metals in CO<sub>2</sub>-free and in CO<sub>2</sub>-containing acid solutions,

\* Corresponding author.

including the possible influence of surface topography, working with smooth and rough electrode surfaces.

## 2. Experimental

Runs were made using four different working electrodes (we), namely smooth polycrystalline (pc) Rh, rhodized (rd) Rh, smooth polycrystalline (pc) Pt and columnar structured (cs) Pt. Electrochemical roughening, an electrochemical technique which has been described extensively in previous publications [14], was employed to prepare the cs-Pt we. The procedure consisted basically of the accumulation of a thick hydrous Pt oxide layer built up by applying a fast square wave potential routine to a pc-Pt electrode in acid, followed by electrochemical reduction of the hydrous Pt oxide layer by a linear potential scan. The value of  $R$ , the roughness factor of the cs-Pt we, was defined by the H-atom voltammetric charge ratio involving the charge measured before divided by the charge determined after cs-Pt formation [14]. For these electrodes values of  $R$  up to 70 were used.

Preparation of the rd-Rh we was done by electrolysis from a 2%  $\text{RhCl}_3$  in 0.1 M HCl aqueous solution. For these electrodes the value of  $R$  was in the range  $10 \leq R \leq 33$ . In this case,  $R$  was determined from the H-electroadsorption charge ratio measured at the voltammetric current minimum which appeared between the H-electrosorption current peak potential and the HER threshold potential [15]. The value of  $q_{\text{H}}$ , the charge of H adatoms evaluated by this procedure, was a fraction of the H-atom monolayer charge [15], i.e.  $q_{\text{H}} = 0.59$  monolayer, where the H-atom monolayer charge density was taken as  $q_{\text{H, ml}} = 0.210 \text{ mC cm}^{-2}$ .

The we potential  $E$  was measured against a  $\text{Hg}|\text{Hg}_2\text{SO}_4|0.5 \text{ M H}_2\text{SO}_4$  reference electrode (MSE) ( $E_{\text{MSE}}/(\text{vs. SHE}) = 0.660$  at  $25^\circ\text{C}$ ), although in the text all potentials are given on the standard hydrogen electrode scale (SHE). A Pt gauze was employed as counterelectrode.

The electrolyte solution was aqueous 0.5 M  $\text{H}_2\text{SO}_4$  prepared from 98%  $\text{H}_2\text{SO}_4$  (Merck, p.a.) and Milli-Q<sup>+</sup> water. Reduced  $\text{CO}_2$  adsorbates were produced by keeping the we immersed in the  $\text{CO}_2$ -saturated solution at a potential which was preset somewhere in the H-atom electroadsorption potential range.

The electroformation of  $\text{CO}_2$  adsorbates and their subsequent electro-oxidation were studied on Rh in a way similar to that previously reported for rough Pt [6]. Accordingly, the we was potential cycled between 0.01 V and 1.46 V in 0.5 M  $\text{H}_2\text{SO}_4$ ; then, after saturating the solution with  $\text{CO}_2$ , the potential was stepped to  $E_{\text{ad}}$  for different adsorption times  $t_{\text{ad}}$ . Adsorption equilibrium was reached for  $t_{\text{ad}} = 10$  min. Finally, the potential was stepped to 0.26 V. Subsequently, a voltammetric scan from 0.26 V to 1.15 V was run in 0.5 M  $\text{H}_2\text{SO}_4$  at potential scan rates in the

range  $0.001 \text{ V s}^{-1} \leq v \leq 0.20 \text{ V s}^{-1}$ . Voltammetry and potentiostatic polarization data were obtained with conventional circuitry. Voltammograms and polarization curves are displayed as  $E$  vs.  $j$  plots, where  $j$  stands for the real current density.

All the experiments were performed at  $25^\circ\text{C}$ .

## 3. Results

### 3.1. Voltammetric data

As reported in previous publications [6,7], r- $\text{CO}_2$  adsorbates on Pt in acids are formed in the range  $0 \text{ V} \leq E \leq 0.4 \text{ V}$  which is related to the formation of H-adatoms (region I). The voltammogram for the electro-oxidation of r- $\text{CO}_2$  on pc- and cs-Pt electrodes in aqueous 0.5 M  $\text{H}_2\text{SO}_4$  exhibits a complex current peak which is scarcely sensitive to the we topography (Fig. 1). This current peak, which is observed even at the highest  $v$  covered by this work, indicates the presence of at least two r- $\text{CO}_2$  adsorbates. The relative current contribution of these adsorbates depends on  $E_{\text{ad}}$ ,  $t_{\text{ad}}$  and  $v$ .

Electro-oxidation voltammograms of r- $\text{CO}_2$  adsorbates formed on cs-Pt for constant  $E_{\text{ad}}$  and increasing  $t_{\text{ad}}$  (Fig. 1) show that  $E_{\text{p}}$ , the current peak potential, moves positively and  $q_{\text{ox}}$ , the electro-oxidation real charge density, increases with  $t_{\text{ad}}$ . Further, a current peak in the potential range 0.7–0.8 V is observed. The value of  $q_{\text{ox}}$  resulting from these voltammograms reaches a maximum value when  $E_{\text{ad}} \approx 0.12 \text{ V}$  (Fig. 2).

For Rh, similar experiments indicate that in this case region I extends over the range  $0 \text{ V} \leq E \leq 0.3 \text{ V}$  where the H-atom electroadsorption reactions take place. For values

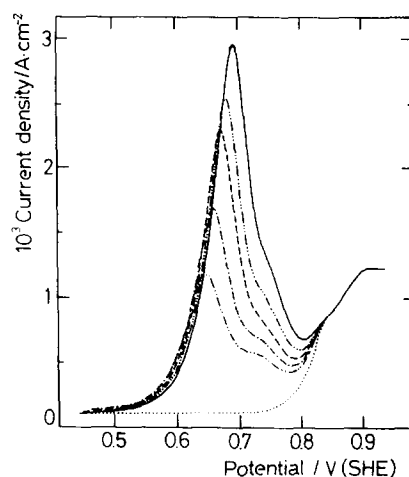


Fig. 1.  $j/E$  voltammogram of the electro-oxidation of r- $\text{CO}_2$  adsorbates formed on cs-Pt ( $R = 26$ ) at  $v = 0.05 \text{ V s}^{-1}$ ,  $E_{\text{ad}} = 0.06 \text{ V}$ ;  $t_{\text{ad}}$  is (—) 300 s, (····) 120 s, (---) 60 s, (-·-·) 30 s, (- - -) 15 s (····) baseline voltammogram in the absence of  $\text{CO}_2$ . Current densities are referred to the electrode real surface area before the columnar structure preparation process;  $25^\circ\text{C}$ .

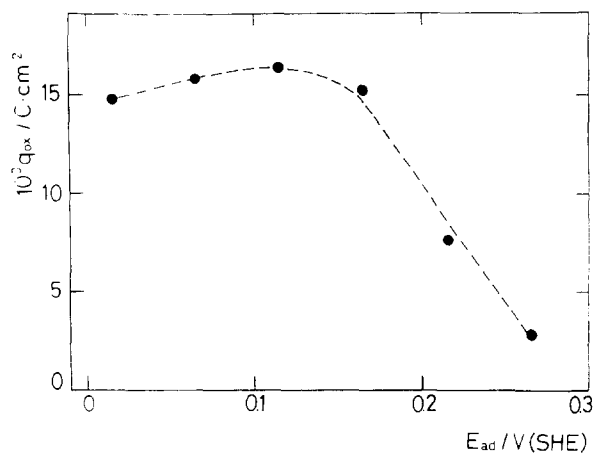


Fig. 2. r-CO<sub>2</sub> electro-oxidation charge density vs.  $E_{ad}$ ;  $t_{ad} = 300$  s, cs-Pt electrode ( $R = 70$ ). Charge densities are referred to the real area of the Pt electrode before the columnar structure preparation; 25°C.

of  $E_{ad}$  in the range  $0.01 \text{ V} \leq E_{ad} \leq -0.15 \text{ V}$ , and for  $t_{ad}$  values in the range  $0 \text{ s} \leq t_{ad} \leq 300 \text{ s}$ , the electroadsorption of CO<sub>2</sub> begins at potentials below approx. 0.1 V, in good agreement with data previously reported from radio-tracer measurements [9].

Single sweep electro-oxidation voltammograms for r-CO<sub>2</sub> adsorbates on pc-Rh run from  $E_{ad}$  upwards (Fig. 3) are, in principle, comparable with those obtained for cs-Pt (Fig. 1). However, for Rh, the electro-oxidation potential of r-CO<sub>2</sub> adsorbates, which starts at ca. 0.2 V below that of Pt, extends over a range which largely overlaps the O-electroadsorption potential range.

The r-CO<sub>2</sub> main electro-oxidation voltammetric peak on pc-Rh becomes sharp at low values of  $v$  (Fig. 3). For  $E_{ad} = -0.14 \text{ V}$  and  $t_{ad} = 200 \text{ s}$ , the voltammogram shows

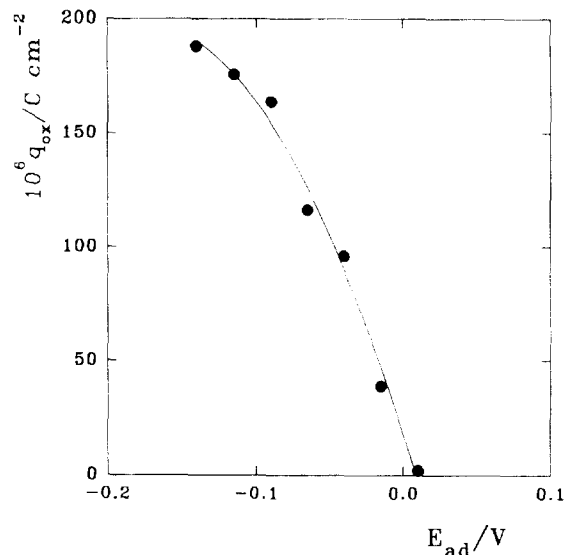


Fig. 4. r-CO<sub>2</sub> electro-oxidation charge density vs.  $E_{ad}$ ;  $t_{ad} = 300$  s, pc-Rh electrode, 0.5 M H<sub>2</sub>SO<sub>4</sub>, 25°C.

a negative shift of  $E_p$  as  $v$  is decreased from  $0.01 \text{ V s}^{-1}$  to  $0.001 \text{ V s}^{-1}$  (Fig. 3). A similar shift of  $E_p$  has also been observed for all Pt electrodes [6]. At a constant  $v$ , the value of  $E_p$  for pc-Rh is very close to that already found for cs-Pt [7].

Otherwise, to attain for pc-Rh a value of  $q_{ox}$  similar to that resulting from cs-Pt, it was necessary to set  $E_{ad} < 0 \text{ V}$  as it results from comparison of data shown in Figs. 2 and 4, after considering that for cs-Pt,  $R = 70$ . Likewise, the value of  $q_{ox}$  increases as  $E_{ad}$  is decreased (Fig. 4) showing that for  $E > 0.06 \text{ V}$ , almost no formation of r-CO<sub>2</sub> species takes place on pc-Rh in acid.

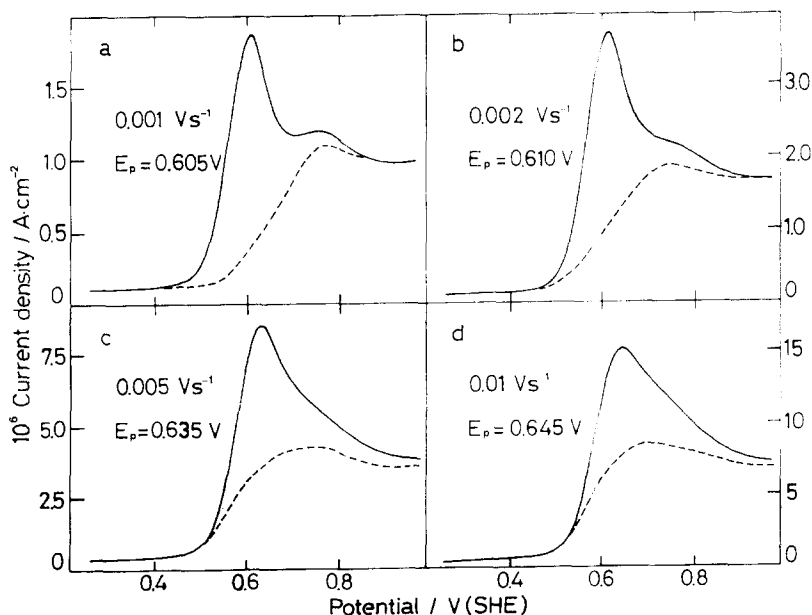


Fig. 3. Electro-oxidation voltammograms of r-CO<sub>2</sub> adsorbates run at different  $v$ ;  $E_{ad} = -0.14 \text{ V}$ ,  $t_{ad} = 200 \text{ s}$ . Dashed lines refer to CO<sub>2</sub>-free 0.5 M H<sub>2</sub>SO<sub>4</sub>; pc-Rh electrode, 25°C.

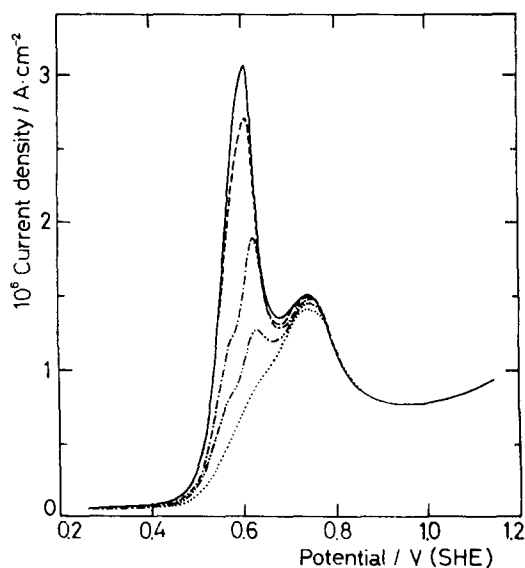


Fig. 5. Electro-oxidation voltammograms of r-CO<sub>2</sub> adsorbates formed at different  $E_{ad}$ ;  $v = 0.001 \text{ V s}^{-1}$ ,  $t_{ad} = 300 \text{ s}$ ;  $E_{ad}$  is (—)  $-0.14 \text{ V}$ , (---)  $-0.09 \text{ V}$ , (- - -)  $-0.04 \text{ V}$ , (- · - ·)  $-0.015 \text{ V}$ . The dotted line refers to the absence of CO<sub>2</sub>; pc-Rh electrode,  $0.5 \text{ M H}_2\text{SO}_4$ ,  $25^\circ\text{C}$ .

Furthermore, the voltammogram at  $v = 0.001 \text{ V s}^{-1}$  for the electro-oxidation of r-CO<sub>2</sub> adsorbates formed at values of  $E_{ad}$  in the range  $-0.015 \text{ V} \leq E_{ad} \leq -0.14 \text{ V}$  and  $t_{ad} = 300 \text{ s}$  on pc-Rh, shows that in the potential range of the main current peak, a first current contribution appears as a shoulder at ca  $0.57 \text{ V}$ , and a second contribution appears at ca  $0.61 \text{ V}$  (Fig. 5). These two contributions involve a charge value equivalent to values of  $\theta_{\text{CO}_2}$ , the degree of surface coverage by r-CO<sub>2</sub> species, in the range  $0 \leq \theta_{\text{CO}_2} \leq 1$ . The value  $\theta_{\text{CO}_2} = 1$  was taken arbitrarily for  $q_{\text{ox}} = 0.210 \text{ mC cm}^{-2}$ . It should be noted that in these experiments no current peak splitting can be distinguished either for  $\theta_{\text{CO}_2} \rightarrow 1$  or for  $v > 0.001 \text{ V s}^{-1}$ .

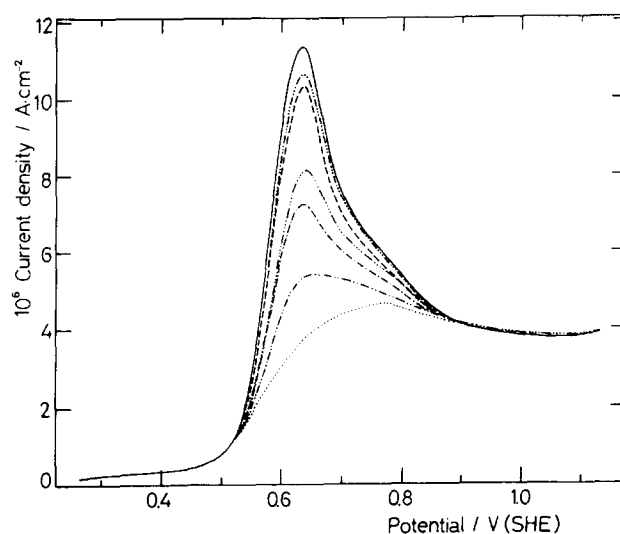


Fig. 6. Electro-oxidation voltammograms of r-CO<sub>2</sub> adsorbates formed at different  $E_{ad}$ ;  $v = 0.005 \text{ V s}^{-1}$ ,  $t_{ad} = 300 \text{ s}$ ;  $E_{ad}$  is (—)  $-0.14 \text{ V}$ , (- · - ·)  $-0.115 \text{ V}$ , (- - -)  $-0.09 \text{ V}$ , (- · · · ·)  $-0.065 \text{ V}$ , (- - -)  $-0.04 \text{ V}$ , (- · - ·)  $-0.015 \text{ V}$ . Dotted line refers to the absence of CO<sub>2</sub>; pc-Rh electrode,  $0.5 \text{ M H}_2\text{SO}_4$ ,  $25^\circ\text{C}$ .

For r-CO<sub>2</sub> electro-oxidation on pc-Rh the value of  $E_p$  also depends on  $E_{ad}$  (Figs. 5 and 6), and from the corresponding values of  $q_{\text{ox}}$  it results that the largest  $\theta_{\text{CO}_2}$  appears when  $E_{ad} = -0.14 \text{ V}$  and  $t_{ad} = 300 \text{ s}$ . These results are in contrast with those already reported for Pt, where the largest value of  $\theta_{\text{CO}_2}$  was found for  $E_{ad} = 0.1 \text{ V}$  [7].

### 3.2. Polarization curves for the HER at Pt and Rh

The distinct features of r-CO<sub>2</sub> adsorbates formed on Rh and Pt in aqueous  $0.5 \text{ M H}_2\text{SO}_4$  were also reflected through their influence on the stationary HER polarization curves at both pc- and rd-Rh and pc- and cs-Pt electrodes.

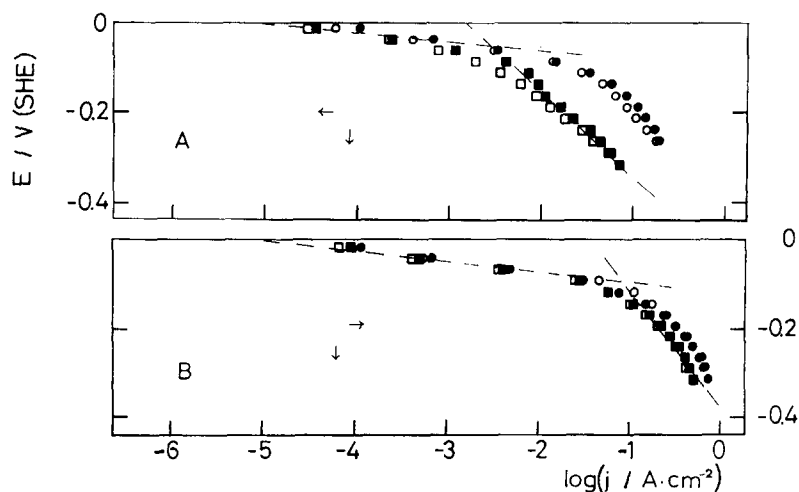


Fig. 7. (a) Tafel plots for the HER on pc-Pt in the presence and absence of CO<sub>2</sub> in solution. (●) From  $0.4 \text{ V}$  to  $-0.3 \text{ V}$ , N<sub>2</sub> saturated solution. (○) From  $-0.3 \text{ V}$  to  $0.4 \text{ V}$ , N<sub>2</sub> saturated solution. (■) From  $0.4 \text{ V}$  to  $-0.35 \text{ V}$ , CO<sub>2</sub> saturated solution. (□) From  $-0.35 \text{ V}$  to  $0.4 \text{ V}$ , CO<sub>2</sub> saturated solution. (b) Tafel plots for the HER on cs-Pt ( $R = 75$ ) in the presence and in the absence of CO<sub>2</sub> in solution. (●) From  $0.4 \text{ V}$  to  $-0.3 \text{ V}$ , N<sub>2</sub> saturated solution. (○) From  $-0.3 \text{ V}$  to  $0.4 \text{ V}$ , N<sub>2</sub> saturated solution. (■) From  $0.4 \text{ V}$  to  $-0.35 \text{ V}$ , CO<sub>2</sub> saturated solution. (□) From  $-0.35 \text{ V}$  to  $0.4 \text{ V}$ , CO<sub>2</sub> saturated solution. Current densities are referred to the real area of the Pt electrode before the columnar-structure preparation process;  $0.5 \text{ M H}_2\text{SO}_4$ ,  $25^\circ\text{C}$ .

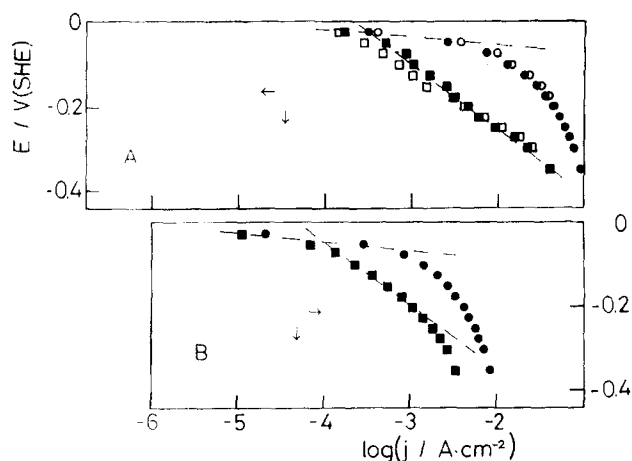


Fig. 8. (a) Tafel plots for the HER on pc-Rh in the presence and in the absence of  $\text{CO}_2$  in solution. (●) From 0.4 V to  $-0.3$  V,  $\text{N}_2$  saturated solution. (○) From  $-0.3$  V to 0.4 V,  $\text{N}_2$  saturated solution. (■) From 0.4 V to  $-0.35$  V,  $\text{CO}_2$  saturated solution. (□) From  $-0.35$  V to 0.4 V,  $\text{CO}_2$  saturated solution. (b) Tafel plots for the HER on rd-Rh in the presence and in the absence of  $\text{CO}_2$  in solution. (●) From 0.4 V to  $-0.3$  V,  $\text{N}_2$  saturated solution. (■) From 0.4 V to  $-0.35$  V,  $\text{CO}_2$  saturated solution.; 0.5 M  $\text{H}_2\text{SO}_4$ , 25°C.

In  $\text{CO}_2$ -free solution and in the absence of r- $\text{CO}_2$  adsorbates, the stationary  $E$  vs.  $\log j$  plot for either pc- (Fig. 7(A)) or cs-Pt (Fig. 7(B)) can be described in terms of two distinguishable potential ranges (regions II and III). Region II, in the range  $0 \text{ V} \leq E \leq -0.1 \text{ V}$ , corresponds to the potential range where the HER takes place. It is characterized by the Tafel slope  $b_T = -0.030 \text{ V decade}^{-1}$ . Region III from  $E < -0.1 \text{ V}$  downwards, involves the HER influenced by the formation of  $\text{H}_2$  bubbles and, in this region  $b_T \approx -0.180 \text{ V decade}^{-1}$ .

Similar polarization curves run for pc-Pt in  $\text{CO}_2$ -saturated solution show a decrease in current in regions II and III compared with those polarization curves recorded in  $\text{CO}_2$ -free solution. On the assumption that the decrease in cathodic current is caused by r- $\text{CO}_2$  adsorbate surface blockage, this effect for  $E < -0.1 \text{ V}$  would appear when  $\theta_{\text{CO}_2} = 0.82$ . This figure for  $\theta_{\text{CO}_2}$  agrees fairly well with that previously reported for both pc- and cs-Pt [6], but it is smaller than that resulting from rd-Rh under comparable conditions.

For cs-Pt immersed in  $\text{CO}_2$ -saturated solution the small shift in the HER polarization curve would correspond to  $\theta_{\text{CO}_2} \approx 0.25$ , a figure which contrasts with  $\theta_{\text{CO}_2} = 0.85$ , the saturation value of  $\theta_{\text{CO}_2}$  previously reported [6,7]. This apparent discrepancy in  $\theta_{\text{CO}_2}$  for pc- and cs-Pt suggests that for the latter, under stationary conditions, only a fraction of the overall surface is accessible to reactants. Presumably this fraction corresponds to tip domains of the columnar topography, i.e. to a fraction of the true electroactive surface [16].

The HER stationary polarization curve for Rh electrodes (Fig. 8) in  $\text{CO}_2$ -free solution involves two distinguishable regions as well. The polarization curve in region II, i.e.  $0 \text{ V}$  to  $-0.1 \text{ V}$ , fits a reasonable Tafel relationship

with  $b_T \approx -0.030 \text{ V decade}^{-1}$ . Finally, in region III, which covers from  $-0.1 \text{ V}$  downwards, the polarization curve also exhibits a rather poor Tafel behaviour with  $b_T \approx -0.180 \text{ V decade}^{-1}$ .

For both pc-Rh (Fig. 8(A)) and rd-Rh (Fig. 8(B)) electrodes in  $\text{CO}_2$ -saturated solution, it appears that, at a constant  $E$ , polarization curves shift towards smaller values of  $j$  compared with those obtained in  $\text{CO}_2$ -free solution, and region II tends to approach a single straight line with the single slope  $b_T \approx -0.120 \text{ V decade}^{-1}$ . Seemingly, r- $\text{CO}_2$  adsorbates on Rh, in contrast to Pt, modify considerably the kinetics of the HER for  $E < -0.05 \text{ V}$ . For Rh, the value of  $\theta_{\text{CO}_2}$  for  $E < -0.1 \text{ V}$ , which would be associated with the change in behaviour of the polarization curve, is  $\theta_{\text{CO}_2} > 0.94$ .

Finally, polarization curves resulting from either decreasing or increasing the potential stepwise tend to coincide, although the current obtained in region I is generally higher when  $E$  is shifted positively.

#### 4. Discussion

##### 4.1. Possible adsorbates formed on Pt and Rh from $\text{CO}_2$ dissolved in 0.5 M $\text{H}_2\text{SO}_4$

The anodic stripping voltammograms of r- $\text{CO}_2$  adsorbates and the influence these adsorbates exert on the HER on Rh and Pt in aqueous 0.5 M  $\text{H}_2\text{SO}_4$  show some noticeable differences, which can be considered by looking first at the characteristics of r- $\text{CO}_2$  adsorbates on Rh and Pt.

The formation of r- $\text{CO}_2$  adsorbates from the  $\text{CO}_2$ -containing solution on both Pt and Rh results from the interaction between the metal surface covered either partially or completely by H-adatoms, and  $\text{CO}_2$  in the solution, although the presence of H-adatoms appears to be a necessary but not a sufficient condition for anchoring  $\text{CO}_2$  on these metals [17]. However, the reactivity of  $\text{CO}_2$  differs depending on whether strongly or weakly bound H-adatoms are involved [6,7], as can be deduced from the anodic stripping peak multiplicity for the corresponding adsorbates [7,18]. Therefore, although seemingly the behaviour of Rh and Pt for r- $\text{CO}_2$  adsorbate formation is qualitatively comparable, the potential for the highest yield of r- $\text{CO}_2$  adsorbates on Rh is more negative than that for Pt, and the electro-oxidation of r- $\text{CO}_2$  adsorbates on Rh is less clearly defined because of the overlapping of the early stages of O-electroadsorption which occurs at potentials below that for Pt.

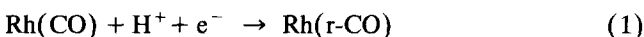
However, anodic stripping voltammograms of r- $\text{CO}_2$  adsorbates on Rh in acid recorded at  $0.001 \text{ V s}^{-1}$  make possible the distinction of at least two forms of r- $\text{CO}_2$  adsorbate as on Pt [6]. For the latter, r- $\text{CO}_2$  adsorbates have been described as ensembles consisting of Pt sites, H-adatoms and trapped  $\text{CO}_2$  species [6]. The electro-oxidation of these ensembles produces in part adsorbed CO

species, as shown recently by “in situ” FTIR spectroscopy [19]. Adsorbed species of the same type should be related to the current contribution which appears in r-CO<sub>2</sub> electro-oxidation on Rh in acid [9].

Otherwise, the fact that the highest value for  $\theta_{\text{CO}_2}$  on Rh is obtained at values of  $E_{\text{ad}}$  more negative than that for Pt, i.e. at values of  $E_{\text{ad}}$  where the HER already takes place, and the ability of Rh to break the CO bond to catalyse hydrogenation reactions [10,11], suggest that the r-CO<sub>2</sub> adsorbates formed on Rh differ from those produced on Pt. Furthermore, the negative shift of the value of  $E_{\text{ad}}$  related to the maximum value of  $\theta_{\text{CO}_2}$  correlates with the fact that sulphate anions are more strongly bonded to Rh than to Pt [20]. Therefore, for Rh the formation itself of H-adatoms required for H-bond-linked CO<sub>2</sub> adsorbate formation takes place in a potential range which is shifted negatively with respect to that for Pt.

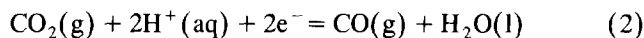
From analysis of the voltammograms, it is likely that r-CO<sub>2</sub> adsorbates on Rh will involve some new adsorbed species produced at relatively high negative potentials where the formation of precursors involved in the electroreduction of CO<sub>2</sub> itself may take place. This reaction would either interfere or compete with the HER. This new adsorbed species could be related to those adsorbed residues involved in the electro-oxidation of formic acid as the cyclic voltammograms of r-CO<sub>2</sub> and CHO<sub>2</sub>H adsorbates on Rh tend to resemble each other [21–23]. In fact, the electro-oxidation current contribution found at lower potentials, which is enhanced when  $E < -0.05$  V, can be related to those current peaks recorded for the voltammetric electro-oxidation of CO and CHO<sub>2</sub>H on Rh in acid [9]. Thus, for both pc-Rh [24] and rd-Rh [22] the voltammetric oxidation of adsorbed CO exhibits a single sharp anodic current peak covering a potential range which largely overlaps the initial stages of Rh(OH) formation [24]. Likewise, the electro-oxidation of CHO<sub>2</sub>H on Rh also involves the formation of a main adsorbate which is electro-oxidized in the same potential range related to the r-CO<sub>2</sub> adsorbate [22,23]. Therefore, it seems reasonable to admit that the presence of two closely located current peaks for (r-CO<sub>2</sub>) electro-oxidation on Rh could be related to a CO-type adsorbate as the tightly bound C-containing adsorbed residue, and a weakly bound r-CO<sub>2</sub> adsorbate.

However, for Rh at  $E < -0.05$  V (region II), the CO adsorbate can also be partially electroreduced according to a reaction such as



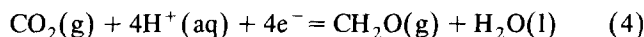
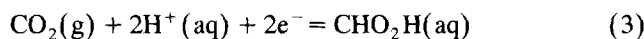
Reaction (1) would produce a rather large coverage of the Rh surface by the r-CO adsorbate, i.e. an adsorbate which may be considered as a precursor for the formation of organics from the electroreduction of CO<sub>2</sub> on Rh. In fact, the voltammetric electro-oxidation of (r-CO) (Fig. 3) tends to be closer to that of species resulting from CHO<sub>2</sub>H adsorption on Rh rather than on other molecules such as methanol [9].

In principle, the preceding interpretation can be supported by thermodynamic data. Thus, the potential range related to the formation of CO adsorbates in region I can be compared with the half-cell potential for the reduction of CO<sub>2</sub> to CO according to [25,26]



which is  $E_r$  (vs. SHE) =  $-0.104$  V. Therefore, as has been concluded recently for Pt and Pd [3,13], the formation of r-CO<sub>2</sub> as a co-adsorbate for  $E > -0.10$  V should be also considered as an underpotential electroadsorption on Rh, although the process is positively shifted for Pt compared with Rh.

The formation of r-CO species and reduced species from r-CO<sub>2</sub> in region II, for  $E < -0.1$  V, becomes thermodynamically feasible as the half-cell potentials for the formation of species such as CHO<sub>2</sub>H and CH<sub>2</sub>O, from CO<sub>2</sub> and H<sup>+</sup>-ion according to the following reactions



are  $E_r$  (vs. SHE) =  $-0.114$  V [25,26], and  $-0.028$  V [26,27] respectively. For reaction (3) the value  $E_r$  (vs. SHE) =  $-0.196$  V has also been reported [27]. It should be noted that a change in the phase of the products would change slightly the value of  $E_r$  for reactions (3) and (4). Nevertheless, although the above values of  $E_r$  for the various CO<sub>2</sub>-containing species are small, overpotentials on Rh and Pt are probably larger owing to the formation of adsorbed intermediates on the electrode surface.

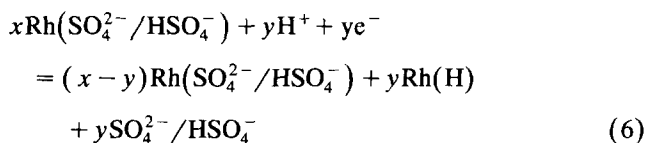
#### 4.2. The kinetics and probable mechanism of the HER on Rh in CO<sub>2</sub>-containing aqueous 0.5 M H<sub>2</sub>SO<sub>4</sub>

At a constant H<sub>2</sub> gas pressure, H<sup>+</sup>-ion activity and temperature, the potential determining reaction for Rh and Pt in acid solution at zero current density (cd),



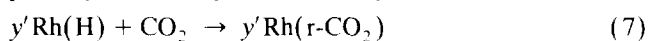
is in equilibrium. For these metals reaction (5) proceeds through the reversible electroadsorption of H-atoms which takes place in region I, whereas the HER occurs in region II.

Let us first consider those processes taking place in region I, i.e. in the H-adatom reversible electroadsorption potential range. In CO<sub>2</sub>-free acid solution, the Rh surface in region I is largely covered by SO<sub>4</sub><sup>2-</sup>/HSO<sub>4</sub><sup>-</sup> ions which adsorb reversibly on Rh in acid [20,28]. Then, H-adatom electrochemical formation would involve the following competitive potential-dependent adsorption equilibrium:

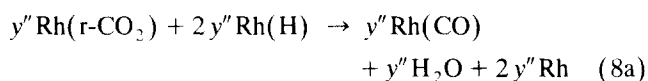


where the parentheses stand for adsorbed species, and  $x$  and  $(x - y)$  are the fractions of the Rh surface covered by sulphate anions, and  $y$  is the fraction of Rh covered by H-adatoms, respectively, with the ratio  $x/y$  decreasing as the applied potential is shifted negatively.

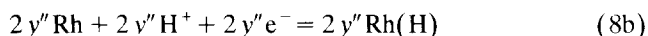
However, in a CO<sub>2</sub>-containing solution, r-CO<sub>2</sub> adsorbates are formed on an electrode surface which is already partially covered by H-adatoms by a reaction such as



where  $y' < y$ . Furthermore, in region I a reduction in (r-CO<sub>2</sub>) species by H-adatoms appears to be possible yielding CO-type adsorbed species. This process can formally be represented by



and H-adatoms are replenished according to the reaction



where  $y'' < y' < y$ , and  $y'$  and  $y''$  denote the fraction of the Rh surface covered by (r-CO<sub>2</sub>) and (CO) respectively. Reaction (8b) would be influenced by anion adsorption as indicated by reaction (6).

For the sake of simplicity, the r-CO<sub>2</sub> adsorbate ensemble could be represented as (2HCO<sub>2</sub>) [29] and it decomposes on Rh yielding CO-type adsorbates as described for Pt and Pd [17] in the same solution. Therefore, in the presence of CO<sub>2</sub> three types of adsorbate would coexist on Rh in the acid solution in region I, namely (H), (r-CO<sub>2</sub>) and (CO), the latter being the dominant species, as can be concluded from FTIRS data [17]. These adsorbates would account for the presence of two current contributions owing to (r-CO<sub>2</sub>) and (CO) in the anodic stripping voltammogram depicted in Fig. 5, which has also been observed for Pd and Pt [17]. Voltammetric data also show a large overlapping of the electro-oxidation potential range of these adsorbates [22,23].

Let us consider now the HER which takes place in region II. In the absence of CO<sub>2</sub>, the HER polarization curves for both Rh and Pt fit Tafel lines, the slope of which depends on the cd range. Thus, in the low cd range,  $b_T \approx -0.030 \text{ V decade}^{-1}$ , i.e. a value very close to the  $-2.303 RT/2F$  ratio at 25°C, irrespective of the direction of stepping the potential. Likewise, in the high cd range,  $b_T \approx -0.180 \text{ V decade}^{-1}$ .

The value  $b_T \approx -0.030 \text{ V decade}^{-1}$  has been related to a reaction pathway involving two consecutive steps, namely a fast discharge of H<sup>+</sup> ions followed by a slow combination of two H-adatoms yielding H<sub>2</sub> [30,31]. In this case, a Langmuir adsorption isotherm has been assumed for H-adatoms.

When CO<sub>2</sub> is present in the solution there is an increase in the cathodic overvoltage for the HER, particularly for pc-Pt, and pc-Rh and rd-Rh. In addition, there is a clear change in the Tafel slope for the HER on Rh in the low cd range, whereas the values of  $b_T$  for Pt in the low and high

cd range, and for Rh in the high cd range, appear to be independent of the presence of CO<sub>2</sub>. Unfortunately, at higher cathodic overpotentials ( $E < -0.1 \text{ V}$ ) it is virtually impossible to separate the influence of CO<sub>2</sub> and the interference of H<sub>2</sub> bubbling in the HER polarization curves.

The entire influence of CO<sub>2</sub> on the Tafel plot for the HER is mitigated appreciably on cs-Pt. The influence of CO<sub>2</sub> in this case is probably due to a considerable blockage of the cs-Pt surface leaving only tip domains as active surface areas for the HER. In this case, the absence of hysteresis in the polarization curves run by stepping the potential forwards and backwards would indicate that the surface blockage owing either to (r-CO<sub>2</sub>), (CO) or H<sub>2</sub> in voids remains approximately the same in the entire HER potential range.

The influence of CO<sub>2</sub> on the HER polarization curve for Rh already begins at 0 V, i.e. at a potential lower than that for Pt. In this case, the presence of CO<sub>2</sub> leads to a Tafel region with a considerable increase in  $b_T$  as it approaches  $b_T \approx -2RT/F$  even in the low cd range. These facts are consistent with the shift of the polarization data shown in Figs. 7 and 8. Further, for Rh the maximum  $q_{ox}$  value results for  $E_{ad} = -0.14 \text{ V}$  and  $t_{ad} = 300 \text{ s}$ . Seemingly, at this potential the interference of sulphate anion adsorption on Rh becomes negligible [20], favouring (r-CO) formation. The presence of a high surface coverage of Rh by (r-CO) adsorbates would mean that in region II the HER is hindered, as results from the shift in  $b_T$  from  $-0.030 \text{ V decade}^{-1}$  in the CO<sub>2</sub>-free solution to  $b_T = -0.120 \text{ V decade}^{-1}$  in CO<sub>2</sub>-containing solutions. Following the conventional reaction pathway proposed for the HER under a Langmuir adsorption for adsorbed reaction intermediates, this change in  $b_T$  can be related to a shift in the rate-determining step for the HER from the H-adatom combination step (Tafel step) to the first electron transfer step (Volmer step). This shift is probably favoured by the fact that, as concluded from tracer experiments, the  $j_0$  (Volmer step)/ $j_0$  (Tafel step) ratio is 1 or thereabouts [32].

From the above interpretation it can be concluded that the increase in the degree of surface coverage by (r-CO) on Rh modifies the kinetics and mechanism of the HER by decreasing the degree of surface coverage by those species acting as intermediates in the HER [31], and by shifting the rate-determining step in the HER pathway from the H-adatom combination step to the first electron transfer step.

In conclusion, the difference in the behaviour of Rh and Pt towards their interaction with CO<sub>2</sub> in the electrochemical environment is to some extent comparable with that already found for these metals in contact with CO<sub>2</sub> in the gas phase [33–36].

## 5. Conclusions

The electroadsorption of CO<sub>2</sub> for Pt commences at ca. 0.3 V and attains a maximum at ca. 0.1 V, whereas for Rh it

begins at ca. 0 V and increases steadily to attain the maximum coverage at ca.  $-0.15$  V. This negative shift in the adsorption potential for Rh correlates with the greater adsorbability of sulphate anions on Rh as compared with Pt.

Adsorbed species formed from the underpotential electroadsorption of  $\text{CO}_2$  on Rh and Pt in acid solution can be ascribed to a reduced form of adsorbed  $\text{CO}_2$  and a CO-type adsorbate, the latter appearing as the predominant surface species. For Rh in the HER potential range a new adsorbed species is formed which is probably related to a reduced form of adsorbed CO. Accordingly, there is an indirect effect of sulphate anion adsorption via H-adatoms on the electrochemical behaviour of  $\text{CO}_2$  on Rh and Pt in acid.

The presence of  $\text{CO}_2$  adsorbates on Pt produces an increase in the cathodic overvoltage particularly in the high cd range. The Tafel slope for the HER in the low cd range is  $b_T = -0.030$  V decade $^{-1}$ , irrespective of the presence of  $\text{CO}_2$  in the solution. The Tafel slope for the HER on Rh increases from  $b_T = -0.030$  V decade $^{-1}$  for  $\text{CO}_2$ -free acid solution to  $b_T = -0.120$  V decade $^{-1}$  for  $\text{CO}_2$ -containing solution.

The change in the Tafel slope for the HER on Rh in acid suggests a change in the rate-determining step in the HER pathway. In the absence of  $\text{CO}_2$  a Tafel mechanism under a Langmuir isotherm for the reaction intermediates accounts formally for the HER kinetics, whereas in the presence of adsorbates produced from  $\text{CO}_2$  a Volmer mechanism can explain the kinetics of the system.

## Acknowledgement

This research project was financially supported in part by the CONICET (Argentina) and the CIC of the Province of Buenos Aires, Argentina.

## References

- [1] J. Giner, *Electrochim. Acta*, 8(1963) 857; 9(1964)63.
- [2] I. Taniguchi, in R.E. White, J.O'M. Bockris and B.E. Conway, (Eds.), *Modern Aspects of Electrochemistry*, Vol. 20, Plenum, New York, 1989, Chapter 5.
- [3] Y. Hori, H. Wakebe, T. Tsukamoto and O. Koga, *Electrochim. Acta*, 39(1994)1833.
- [4] J. Paul and C.M. Pradier (Eds.), *Carbon Dioxide Chemistry*, Royal Society of Chemistry, Cambridge, 1994.
- [5] V.E. Kazarinov, V.N. Andreev and G. Ya. Tsyachanaya, *Elektrokhimiya*, 8(1972)927.
- [6] M.L. Marcos, J.M. Vara, J. Gonzalez Velasco and A.J. Arvia, *J. Electroanal. Chem.*, 224 (1987) 189.
- [7] M.L. Marcos, J. Gonzalez Velasco, J.M. Vara, M.C. Giordano and A.J. Arvia, *J. Electroanal. Chem.*, 270(1989)205; 281(1990)257; 287(1990)99.
- [8] A.V. Zakharian, N.V. Ositrova and Yu. B. Vassiliev, *Elektrokhimiya*, 13(1977)1011.
- [9] J. Sobkowski, A. Wieckowski, P. Zelenay and A. Cerwinski, *J. Electroanal. Chem.*, 100(1979)781.
- [10] G.A. Somorjai, *Chemistry in Two Dimensions: Surfaces*, Cornell University Press, London, 1981.
- [11] F. Solymosi, in J. Paul and C.M. Pradier (Eds.), *Carbon Dioxide Chemistry*, Royal Society of Chemistry, Cambridge, 1994, p. 44.
- [12] A.V. Zakharian, N.V. Ositrova and Yu. B. Vassiliev, *Elektrokhimiya*, 12(1976)1854.
- [13] B.I. Podlovchenko, E.A. Kolyadko and S. Lu, *Elektrokhimiya*, 30(1994)670.
- [14] A.C. Chialvo, W.E. Triaca and A.J. Arvia, *J. Electroanal. Chem.*, 146 (1983) 93.
- [15] R. Woods, in A.J. Bard (Ed.), *Electroanalytical Chemistry*, Vol. 9, Marcel Dekker, New York, 1977.
- [16] L. Vásquez, J. Gomez, A.M. Baró, N. García, M.L. Marcos, J. González Velasco, J. M. Vara, A.J. Arvia, J. Presa, A. García and M. Aguilar, *J. Am. Chem. Soc.*, 109 (1987) 1730.
- [17] S. Taguchi, A. Aramata and M. Enyo, *J. Electroanal. Chem.*, 372 (1994) 161.
- [18] M.C. Arévalo, C. Gomis-Bas, E. Pastor, S. González and A.J. Arvia, *Electrochim. Acta*, 37 (1992) 1083.
- [19] M.L. Marcos, J. González Velasco, F. Hahn, B. Beden, C. Lamy and A.J. Arvia, in preparation.
- [20] P. Zelenay, G. Horanyi, C.K. Rhee and A. Wieckowski, *J. Electroanal. Chem.*, 300 (1991) 499.
- [21] A. Capon and R. Parsons, *J. Electroanal. Chem.*, 44 (1973) 239.
- [22] A. Czerwinski, *J. Electroanal. Chem.*, 252 (1988) 189.
- [23] M.L. Marcos, J. Gonzalez Velasco and A.J. Arvia, unpublished results.
- [24] S.A. Bilmes, N.R. de Tacconi and A.J. Arvia, *J. Electroanal. Chem.*, 143 (1983) 179.
- [25] M. Schmidt, in J. Paul and C.M. Pradier (Eds.), *Carbon Dioxide Chemistry*, Royal Society of Chemistry, Cambridge, 1994, p. 27.
- [26] W.M. Ayers, in J. Paul and C.M. Pradier (Eds.), *Carbon Dioxide Chemistry*, Royal Society of Chemistry, Cambridge, 1994, p. 366.
- [27] A.J. Bard, R. Parsons and J. Jordan (Eds.), *Standard Potentials in Aqueous Solutions*, Marcel Dekker, New York, 1985.
- [28] C. Pallota, N.R. de Tacconi and A.J. Arvia, *J. Electroanal. Chem.*, 159 (1983) 201.
- [29] V.E. Kazarinov, V.N. Andreev and A.V. Shlepakov, *Electrochim. Acta*, 34 (1989) 905.
- [30] S. Schuldiner, *J. Electrochem. Soc.*, 107 (1960) 452.
- [31] L. Gao and B.E. Conway, *Electrochim. Acta*, 39 (1994) 681.
- [32] M. Enyo, in B.E. Conway, J. O'M. Bockris, E. Yeager, S.U.M. Khan and R.E. White (Eds.), *Comprehensive Treatise of Electrochemistry*, Vol. 7, Plenum, New York, 1983, Chapter 5, p. 262.
- [33] B.A. Sexton and G.A. Somorjai, *Surf. Sci.*, 71 (1978) 519.
- [34] S.D. Worley, G.A. Mattson and R. Caudill, *J. Phys. Chem.*, 87 (1983) 1671.
- [35] M.F.H. van Tol, A. Gielbert and B.E. Nieuwenhuys, *Appl. Surf. Sci.*, 67 (1993) 166.
- [36] M.F.H. van Tol, A. Gielbert R.M. Wolf, A.B.K. Lie and B.E. Nieuwenhuys, *Surf. Sci.*, 287 (1993) 201.